Available online at http://www.journalcra.com

International Journal of Current Research
Vol. 7, Issue, 12, pp.23542-23550, December, 2015

INTERNATIONAL JOURNAL OF CURRENT RESEARCH

ISSN: 0975-833X

RESEARCH ARTICLE

SYNTHESIS AND CHARACTERIZATION OF SnO-CoO NANOCOMPOSITES BY BOTTOM UP APPROACH AND THEIR EFFICACY FOR THE TREATMENT OF DYES ASSISTED SIMULATED WASTE WATER

Muhammad Saad, *Dr. Hajira Tahir and Fakhra Shaheen

Department of Chemistry, University of Karachi, Pakistan

ARTICLE INFO

Article History:
Received 25th September, 2015
Received in revised form
07th October, 2015
Accepted 09th November, 2015
Published online 21st December, 2015

Key words:

Nanocomposites;
Tartrazine dye,
Adsorption isotherms,
Thermodynamics,
Kinetic model.

ABSTRACT

The current studies emphasises the synthesis of SnO-CoO nanocomposites by bottom up approach adopting sol gel method. These nano particles were effectively employed as nano adsorbent for the treatment of tartrazine (TR) dye assisted simulated waste water under the influence of variable conditions to achieve best adsorption capacity. The effect of adsorbent amount, adsorbate concentration, stay time and pH_{pzc} were studied. Adsorption isotherm models of Langmuir, Freundlich, Dubinin Radushkevich and Temkin were also employed to check the feasibility of the adsorption process. Adsorption capacities 'K_F' of the adsorbent were determined at 298K, 313K and 323K respectively. Thermodynamic studies were conducted and the values of ΔH^o and ΔS^o were found to be 3113.32 J. $mole^{-1}$ and 56.712 $J.mole^{-1}K^{-1}$ respectively. The spontaneity of adsorption process was affirmed by ΔG^o values. The experimental data was also fitted to various kinetic equations to determine rate constant and order of the reaction like pseudo first order and pseudo second order, intraparticles diffusion model, Boyd's kinetics model and Elovich model. The adsorption data represent pseudo second order kinetics is followed with the major mode mass transfer mode to be diffusion. The surface morphology of nanocomposites was studied by SEM and FTIR techniques. Such recycling methods effectively implemented at industrial scale and therefore assess the challenges posed by them in the environment and public health.

***Citation*:** Muhammad Saad, Dr. Hajira Tahir and Fakhra Shaheen, 2015. "Synthesis and characterization of SnO-CoO Nanocomposites by bottom up approach and their efficacy for the treatment of dyes assisted simulated waste water", *International Journal of Current Research*, 7, (12), 23542-23550.

INTRODUCTION

In recent era, the requirement of new materials and their applications are critical. Nanomaterials (NM) are one of the successful choices for such applications. They consist of dimensions of the order of nanometer (10^{-9} m). Their catalytic, optical, electronic and other physical properties are being used in many applications. In twenty first century, the technology advances in days. Due to increasing wealth and covetousness of human being the requirement of new materials and their applications are essential. The scientific community tries to develop new material with innovative applications (Irena *et al*., 2006). Their catalytic, optical, electronic and other physical properties make them one of the most attractive research topics now a day. The physical properties of nano materials are strongly dependent on their size therefore the morphology describes their physical properties.

Corresponding author: Dr. Hajira Tahir,
Department of Chemistry, University of Karachi, Pakistan.

Altering the synthesis method, reagents, capping agent and the pH govern the morphology of the nanoparticles (Baolin *et al*., 2004). Metal nanoparticles are also photostable and do not undergo photo bleaching. This property allows them to be utilized as ideal colour groups for colorimetric sensor design (Yingju *et al*., 2009). Nanomaterials have much improved physical properties than their parent macro substances therefore they are now being employed in sensors which have much improved sensitivity than their parent electrodes. For example nanoparticles modified electrodes have been used for sensitive and selective determination of 17β-estradiol (Lihua *et al*., 2011), hydroquinone (Bin *et al*., 2005), H_2O_2 (Chunbu *et al*., 2005, Abdollah *et al*., 2007), hypoxanthine (Xiaoli *et al*., 2005), thiocyanate (Guang-Feng *et al*., 2004), and brilliant cresyl blue (Mao-Guo *et al.,* 2005). In the present studies, Tin oxide and Cobalt oxide nanocomposites were synthesized by bottomup approach by sol-gel method in which a specific concentration of precursor was reduced by NaOH in solution form to prepare particles of metals. The metals particles were then mixed and separated from the solution. The obtained

precipitate was then kept at 120°C for 15hours in air oven. The precipitate was then kept at about 400°C for 4 hours. Then the nanocomposites were ground in a piston mortar for further homogeneity. They were utilized for the purification of effluent. Dyes are natural or synthetic compounds and they can be used to colour various materials, and have wide industrial applications .They are available in widest ranges for different applications like acids dyes for wool and nylon, direct dyes for cotton, etc. (NIIR board 2004). Due to increasing demands for textile products, dyes and its intermediates have also increased demand, therefore their emissions in effluent water is much increased in recent past. Certain kinds of dyes can be toxic, carcinogenic or mutagenic and can pose as a hazard to health. Therefore the effluent water must be efficiently treated to minimize the dye and colorants. Nanocomposites have efficiently been employed to treat toxic effluent.

The super paramagnetic Poly(acrylic acid) Coated-Fe_3O_4, Hydrolyzed Polyacrylamide Grafted Xanthan Gum and Incorporated Nanosilica, Fe_3O_4-Cu_2O-PANI, Magnetic Multi-Walled Carbon Nanotubes-Fe_3C, graphite oxide-magnetic chitosan, CaO-Fe_2O_3, sodium alginate-coated Fe3O4, chitosan-MgO, Ag/Kaolin, Polyaniline zirconium (IV) silicophosphate (PANI-ZSP) nanocomposites have been effectively used for the treatment of methylene blue, methyl violet, congo red, methyl orange, acid Red, reactive Black 5, malachite green and acid Cyanine 5R dyes (Chunjiao *et al*., 2013; Sumita *et al*., 2014; Juan *et al*., 2014; Wojciech *et al*., 2014; Hamid *et al*., 2013; Nikolina *et al*., 2013; Sushanta *et al*., 2014; Mittal *et al*., 2014, yuvaraj *et al*., 2014; Saeedeh *et al*., 2013[a]; Vinod *et al*., 2014).

There are several methods reported for the preparation of nanoparticles, including attrition, pyrolysis, radiolysis and sol-gel. Sol-gel method is one of the most widely used methods to prepare nanomaterials due to facile procedure and instrumentation (Saeedeh *et al*., 2013[a]; Saeedeh *et al*., 2013[b]; Mirjalili *et al*., 2010; Ferav *et al*., 2013; Nirasttisai *et al*., 2010). The precursor in sol-gel method is a chemical solution which upon chemical reaction forms discrete particles as a result of hydrolysis and poly condensation of metal alkoxides and metal chlorides.

MATERIALS AND METHODS

Cobalt chloride ($CoCl_2.6H_2O$), Tin Chloride ($SnCl_2.2H_2O$), Sodium Hydroxide (NaOH), tartrazine dye (TR) were used in the experimental work. All the materials were of analytical grade and were used as received. Distilled deionized water was used throughout the experimental work.

Synthesis Of SnO-CoO Nano-Composites

The nanocomposites of SnO-CoO were prepared by sol-gel method. About 16.9g of tin chloride dihydrate ($SnCl_2.2H_2O$) was dissolved in 300mL deionized distilled water under constant stirring which was followed by the addition of 3.0g of NaOH pallets. Similarly, 17.8g of Cobalt chloride hexahydrate ($CoCl_2.6H_2O$) were dissolved in 300mL of deionized distilled water under stirring which was followed by the addition of 3.0g of NaOH pallets.

The solutions were mixed under stirring and the obtained precipitates were kept at 120 °C for 15 hours. The slurry was cooled at room temperature and then washed with ethanol several times after that it was dried and then calcinated at 400°C. Finally SnO-CoO nanocomposites were obtained and they were stored in desiccators for the desired work (Gajendiran *et al*., 2014).

Adsorption Experiments

Adsorption experiments were proceeded by utilizing nanocomposites acting as adsorbent. To check the feasibility of adsorption process, laboratory batch mode of studies was conducted. Batch samples were agitated at 200 rpm to facilitate good contact between the dye and the adsorbent. The suspensions were filtered after agitation. The filtrate was tested to determine residual concentration of dye by (T80 UV/VIS) spectrophotometer. Parameters which influence the extent of adsorption such as adsorbate concentration, adsorbent dosage and agitation time were also investigated.

Effect of Variation in Dye Concentration

A series of concentration of dye about 10, 20, 30, 40 and 50ppm was prepared by standard addition method. Then optimum amount of 0.1g of nanosorbent was added into 50 mL of each specified concentration of the dye. After specific time the suspension was filtered to evaluate the dye concentration.

Optimization Of Amount Of Adsorbent

For the determination of amount of adsorbent at which maximum adsorption takes place, 50mL of 20ppm dye solution was taken in a series of Erlenmeyer flask in which amount of 0.1, 0.2, 0.3 and 0.4g were added. The samples were put in shaking incubator for 1hr at 200rpm. The suspensions were then filtered and the absorbances after addition of adsorbent were determined. The optimum amount of adsorbent was evaluated by the decrease in the absorbance of the dye solution.

Effect of Variation in Adsorbent Stay Period

A series of dye solutions with a concentration of 20ppm of dye adding 0.3g amount of adsorbent was agitated at different time intervals of 5 to 60 minutes. After filtration, the optimized stay time for the adsorbent was evaluated by taking the absorbance after suitable time intervals. The stay time for the maximum adsorption was taken as optimized stay time.

pH AT ZERO POINT CHARGE (pH_{zpc})

pH_{zpc} is abbreviated as pH at zero point charge. pH_{zpc} is the pH at which the surface has an overall neutral charge. Above this pH value, species have overall negative charge and below this, species have an overall positive charge. The pH at the point of zero charge of SnO-CoO nanocomposite was measured by using the pH drift method. The pH of 0.005 $mol.dm^{-3}$NaCl solutions was adjusted between 2.18 to 11.80 by adding required amount of 0.1 M HCl or NaOH. Then 0.3 g of adsorbent was added in 25 mL of solution in Erlenmeyer flask

and left at room temperature in dark for 24 and 48 hrs. The graphs of pH drawn were used to determine the points at which the initial and final pH values were equal (Hajira *et al*. 2014). Final pH of the solutions was recorded and results were plotted.

RESULTS AND DISCUSSION

Characterization Of Nanocomposites

The characterization of the prepared nanocomposites was done by Fourier Transformed Infrared Spectroscopy and Scanning Electron Microscopy.

I-Fourier Transformed Infrared Spectroscopy

The FTIR spectrum of SnO-CoO nanocomposites showed prominent absorption peaks at 669cm^{-1}, 1620cm^{-1} and 3373cm^{-1} as shown in Figure 1.

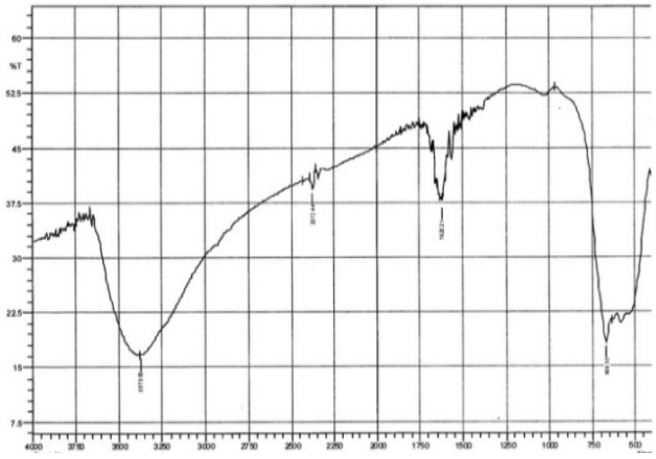

Figure 1. FTIR spectrum of SnO-CoO nanocomposites

The region between 500cm^{-1} to 670cm^{-1} contain many peaks that relates to the stretching and bridging vibrations of oxygen and the hetero atoms (Manigandan *et al*., 2013; Vijayaprasath *et al*., 2013). The absorption peaks at 3374cm^{-1} and 1620 cm^{-1} are mainly due to the vibration of surface OH^- group or adsorbed surface water molecules (Vijayaprasath *et al*., 2013). A very small peak observed at 2372 cm^{-1} is due to some impurity.

Scanning Electron Microscopy

Scanning electron microscope (SEM) is one of the best characterization techniques for the nanoparticles analyses. The scanning electron microscopy was performed on model 6380, JEOL, Japan. The Scanning Electron Micrograph of the prepared nanocomposites is shown in Figure 2.

The scanning electron micrograph indicates that the particles are quite homogenous in nature and the size ranging from 50 - 100nm. The prepared nanocomposites were used in the whole experimentation.

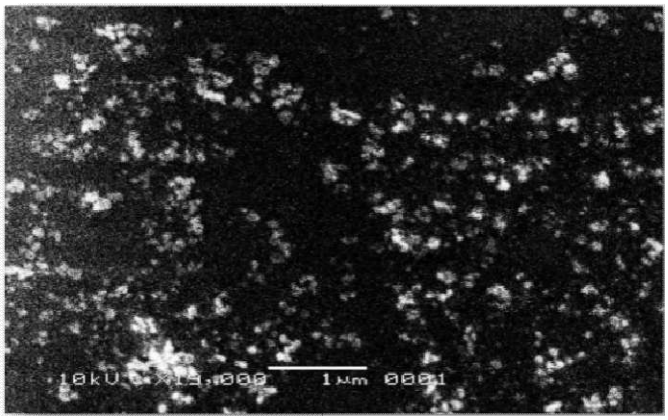

Figure 2.SEM image of the nanocomposites

Adsorption Experiments

Variation In Dye Concentration

In experiment, varying the concentration of the dye from 10 to 50ppm aided in determining the optimum concentration of the dye.

Approximately 0.1g of adsorbent was added in each flask containing 20ppm of dye solution and shaken for the specified period of time. The concentration of dye was observed by spectrophotometer. K_d was also calculated with respect to concentration as shown in the Figure 3.

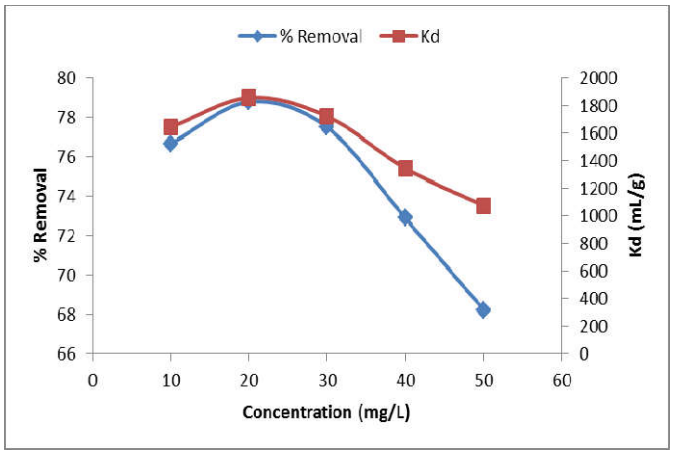

Figure 3. Variation in dye concentration

Effect Of Amount of Adsorbent

The amount of nanocomposites was varied from 0.1g to 0.4g in a system containing 50mL of solution of the tartrazine dye.

The optimum amount of adsorbent was evaluated as 0.3g as it shows the greatest removal tendency of the dye from the solution as shown in Figure 4. Moreover it also revealed that the distribution coefficient gets decreased by increase in the amount of the nanocomposite.

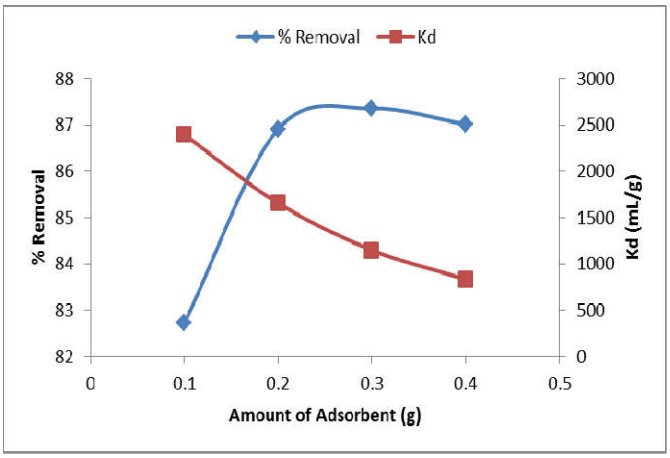

Figure 4. Effect of amount of adsorbent on dye removal and K_d

Variation Of Adsorbent Stay Period

The optimum stay period was evaluated by shaking flasks containing the optimum concentration and optimum amount of nanocomposite for variable intervals of time from 5 to 60 minutes. The optimum stay time for the removal of dye was determined to be 60 minutes. Moreover it is evident from Figure 5 that the distribution coefficient is directly proportional to shaking time period.

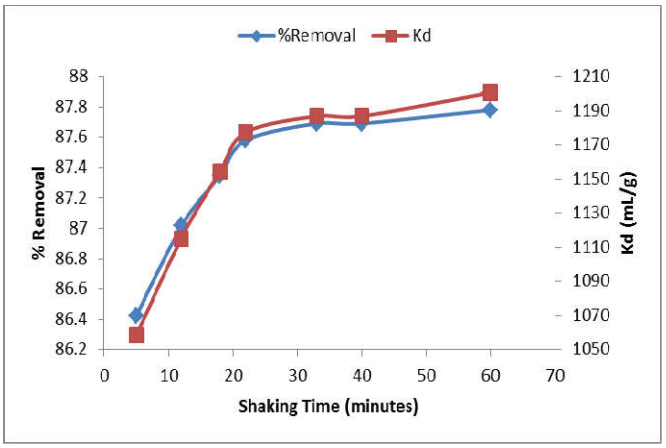

Figure 5. Variation in shaking period

Isotherms Studies

Isotherms are algebraic functions that express relationship between the adsorbed materials with adsorbent (Kumar *et al*., 2013). Studies were made on Freundlich isotherm, Temkin isotherm, Langmuir isotherm, and Dubinin-Radushkevich isotherm and values of respective constants were evaluated.

Freundlich Isotherm

The isotherm supposes an assorted facade of adsorbent with irregular distribution of heat of adsorption over the adsorbent surface and is applicable for mono and multilayered adsorption process (Srivastava *et al*., 2015).This isotherm is used to study the adsorption of dye onto the surface of nanocomposites (Dada *et al*., 2012). The Freundlich model can be expressed as:

$$\log Q_e = \log K_F + \frac{1}{n}\log C_e \quad \text{.....(1)}$$

Where, K_F is a constant that shows the adsorbent capacity. 'n' is the constant that shows surface homogeneity. Values of 'n' and 'K_F' were evaluated via linear plotting log Q_e versus log C_e.

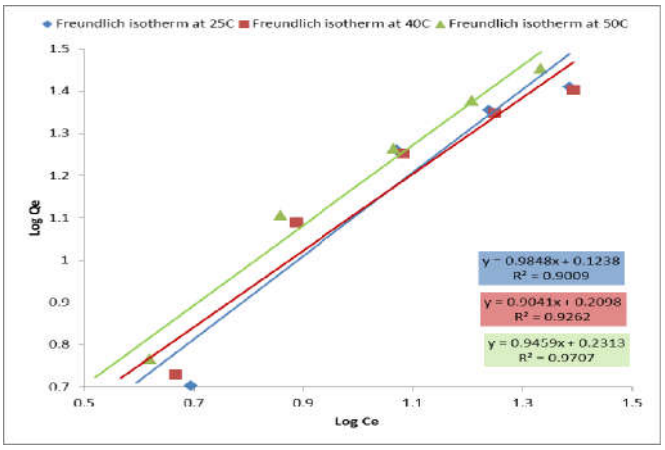

Figure 6. Freundlich isotherms at 25°C, 40°C and 50°C

The values related to the surface homogeneity 'n' were determined to be 1.0154gL^{-1}, 1.1061gL^{-1} and 1.0302gL^{-1} at 298K, 313K and 323K respectively. The adsorption capacities were determined to be 1.3298mg$^{0.0152}$L$^{0.9848}$g^{-1}, 1.6211mg$^{0.0959}$L$^{0.9041}$g^{-1} and 1.7033mg$^{0.0293}$L$^{0.9707}$g^{-1} at 298K, 313K and 323K respectively.

Langmuir Isotherm

The development of a monolayer on the adsorbent façade is described quantitatively by this isotherm, and there is no more adsorption. By this means, this isotherm epitomizes the dye molecules dispersal at equilibrium between the two phases. This isotherm is effective for monolayer adsorption on a surface having finite identical sites. The isotherm supposes constant energies of adsorption onto the exterior and no adsorbate transmigration takes place in the plane of the surface. The following equation was proposed by Langmuir is represented as (Dada *et al*., 2012).

$$Q_e = \frac{Q_o K_L C_e}{1 + K_L C_e} \quad \text{.....(2)}$$

The above equation can be simplified in the linear form as.

$$\frac{1}{Q_e} = \frac{1}{Q_o} + \frac{1}{Q_o K_L C_e} \quad \text{..... (3)}$$

Where: C_e represents the adsorbate concentration at equilibrium (mgL^{-1}) and Q_e represents the adsorbate amount adsorbed at equilibrium per unit mass of the adsorbent (mg.g^{-1}) While Q_o represents the maximum monolayer coverage capacity (mg.g^{-1}) and K_L is the Langmuir isotherm constant (Lmg^{-1}).The values of K_L and Q_o were computed from the slope and intercept of the Langmuir plot of $1/C_e$ versus $1/Q_e$.

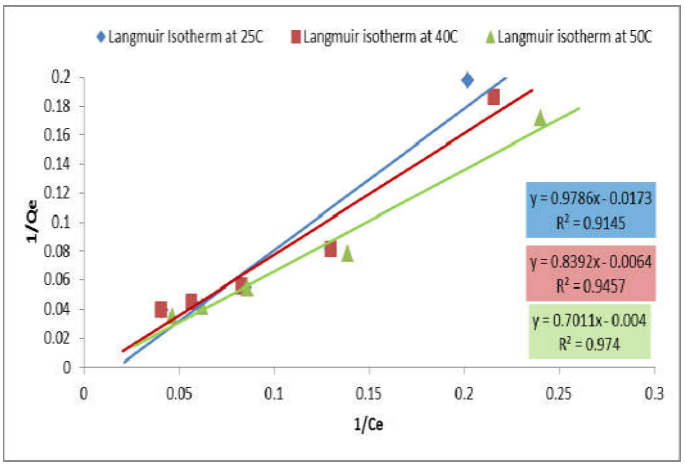

Figure7. Langmuir isotherm at 25°C, 40°C and 50°C

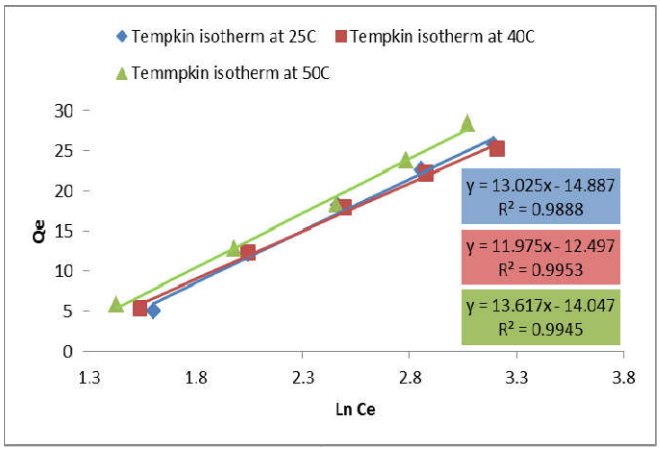

Figure8. Temkin plot of lnC_e versus Q_e at 25°C, 40°C and 50°C

The values of Q_o were calculated to be -57.803 mg.g^{-1}, 156.25mg.g^{-1} and -250mg.g^{-1} at 298K, 313K and 323K respectively. The Langmuir constant K_L were determined to be -0.01768Lmg^{-1}, -0.007626 Lmg^{-1} and 0.005705Lmg^{-1} respectively, indicating that the data does not follow the Langmuir isotherm.

Temkin Isotherm

The variables dealing with adsorbent relations with adsorbate are expressed by this isotherm. This isotherm states that the surface coverage decreases the heat of adsorption by neglecting extreme concentrations. The equation indicates that the variation is considered by an even spreading of binding energies. From the help of equation, a graph of the adsorbed quantity Qe versus lnCe was plotted and the values of respective constants were evaluated from the slope and intercept of the plots. The Temkin model is represented as (Dada *et al*., 2012):

$$Q_e = \frac{RT}{b}\ln(A_T C_e) \quad \ldots\ldots (4)$$

$$Q_e = \frac{RT}{b_T}\ln(A_T) + \frac{RT}{b}[\ln(C]_e) \quad \ldots\ldots (5)$$

$$B = \frac{RT}{b} \quad \ldots\ldots (6)$$

$$Q_e = BlnA_T + BlnC_e \quad \ldots\ldots (7)$$

A_T and b_T are Temkin isotherm binding constants (L.g^{-1}), While R represents the Universal gas constant (8.314Jmol^{-1}K^{-1}) ,T represents Absolute Temperature and B indicates the Constant associated to heat of sorption (Jmol^{-1}).

Dubinin Radushkevich Isotherm

This isotherm explains the adsorption mechanism on a heterogeneous façade with Gaussian energy distribution. This isotherm fits well quite regularly at moderate concentration range and at high activities of solutes (Dada *et al*., 2012).

$$Q_e = (Q_s)e^{-K_{ad}\varepsilon^2} \quad \ldots\ldots (8)$$

$$lnQ_e = lnQ_s - K_{ad}\varepsilon^2 \quad \ldots\ldots (9)$$

Where, Q_e represents the equilibrium adsorbate amount (mg.g^{1}), Q_s represents theoretical saturation capacity of the isotherm (mg.g^{-1}), K_{ad} represents the D–R isotherm constant (mol^2.k^{-1}J^{-2}) and ε is the Dubinin–Radushkevich isotherm constant.

The value of ε is calculated as:

$$\varepsilon = RT\ln[1 + \frac{1}{C_e}] \quad (10)$$

The D-R model is distinctive in a way that this is temperature dependant phenomenon (Dada *et al*. 2012).

From figure 9, the values of D–R isotherm constant 'K_{ad}' were evaluated to be 7.0x10^{-7} mol^{2}k^{-1}J^{-2}, 3.0x10^{-7}mol^{2}k^{-1}J^{-2} and 2.0x10^{-7}mol^{2}k^{-1}J^{-2} at 298K, 313K and 323K respectively with the R^2 values of 0.9931, 0.9993 and 0.9922 respectively.

The values of theoretical isotherm saturation capacity 'Q_s' were evaluated to be 3.542g.g^{-1}, 25.68mg.g^{-1} and 21.73mg.g^{-1} at 298K, 313K and 323K respectively.

Thermodynamic Studies

The thermodynamic parameters such as standard Entropy change ΔS^o (J.mol^{-1}K^{-1}),standard Enthalpy change ΔH^o(kJ.mol^{-1}) and standard Gibbs Free Energy Change ΔG^o(kJ.mol^{-1}) were calculated by using following equations (Zhonghui *et al*. 2014).

$$\Delta G = -RT\ lnK_D \quad \ldots\ldots (11)$$

$$LogK_D = \frac{\Delta S^o}{2.303R} - \frac{\Delta H^o}{2.303RT} \quad \ldots\ldots (12)$$

From the Van't Hoff graph of Log K_d versus T^{-1}, the values of the standard entropy change ΔS^o and standard enthalpy ΔH^o change were determined.

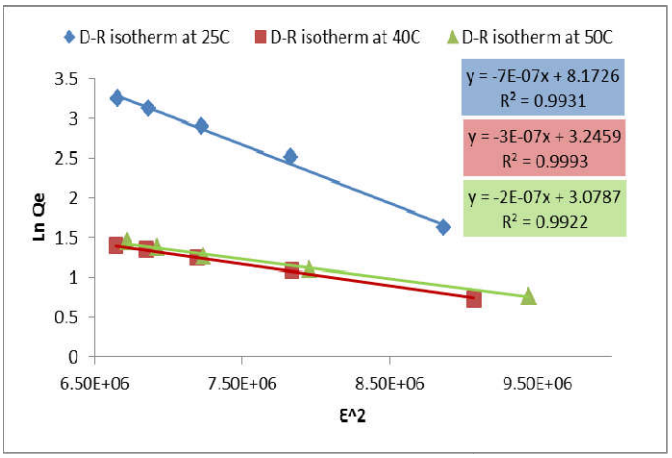

Figure 9. D-R plot of ε^2 versus $\ln Q_e$ at 25°C, 40°C and 50°C

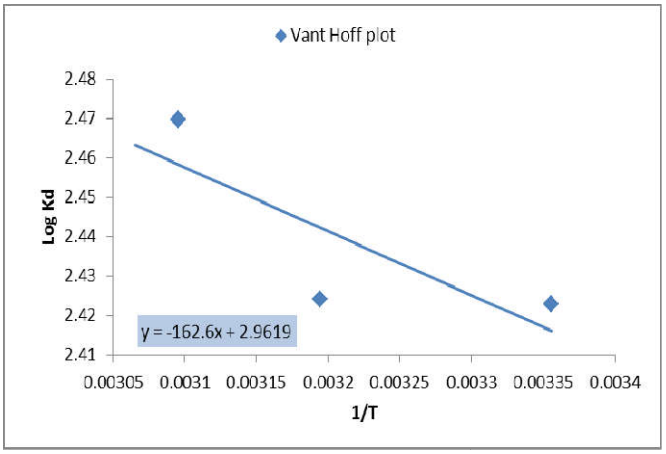

Figure 10. Graph of T^{-1}vs Log K_d

From figure 10, ΔH^o and ΔS^o values were found out to be 3113.3J.mole^{-1} and 56.712J.mole^{-1}K^{-1} respectively. The values of ΔG^o were calculated to be -13.823 kJ.mole^{-1}, -14.526 kJ.mole^{-1} and -15.270kJ.mole^{-1} at 298K, 313K and 323K respectively. The negative ΔG^o values indicate the spontaneous nature of adsorption.

Kinetic Studies

The kinetic study will be carried out by pseudo-first order, pseudo-second order kinetics, Intra-particle Diffusion model, Elovich model and Boyd's kinetic model. The rate constants can be calculated by the plots of pseudo first order and pseudo-second order equations that are represented as.

$$\log(Q_e - Q_t) = \log Q_e - \frac{k_1 t}{2.303} \quad \text{.....(13)}$$

$$\frac{t}{Q_t} = \frac{1}{K_2 Q_e^2} + \frac{t}{Q_e} \quad \text{..... (14)}$$

Where, Q_e is the equilibrium amount adsorbed (mg.g^{-1}), and Q_t represents the adsorbed amount at specified time (mg.g^{-1}) and t is the time (min) taken for the adsorption to occur. While $k_1$and k_2 denote pseudo first order rate constant (min^{-1}) and pseudo second order rate constant (g.mg^{-1}min^{-1}) respectively. Equations (13) and (14) symbolize Pseudo – first and second order rate equations.

I-Pseudo First Order Kinetics

In present studies, the validity of pseudo first order model was confirmed by a plot between Log (Q_e-Q_t) and Time (min).

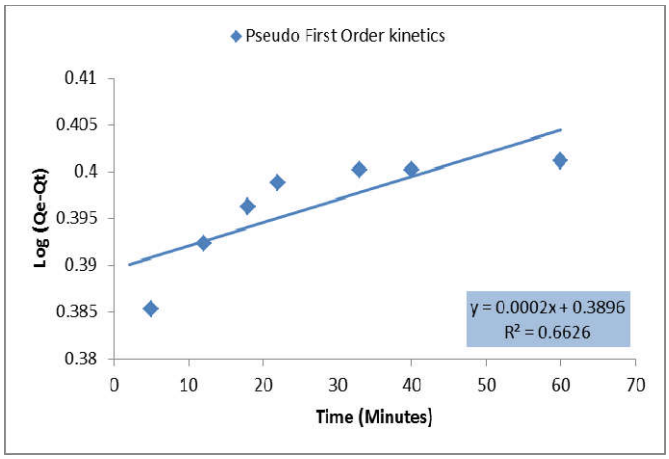

Figure 11. Graph of pseudo first order kinetics

From Figure 11, it can be realized that the adsorption does not strongly follow pseudo first order kinetics. For this kinetic study, a straight line should be obtained but there seemed to be deviation from the straight line showing the deviation. From the figure 11, the value of pseudo first order rate constant 'k_1' was evaluated to be -4.606x10^{-4} min^{-1}.

Pseudo Second Order Kinetics

A plot between t/Q_t and Time (min) was used to confirm the validity of Pseudo second order kinetics. The experimental results were satisfying the second order kinetics as depicted in the Figure 12 as the DATA points were well fit on the straight regression line.

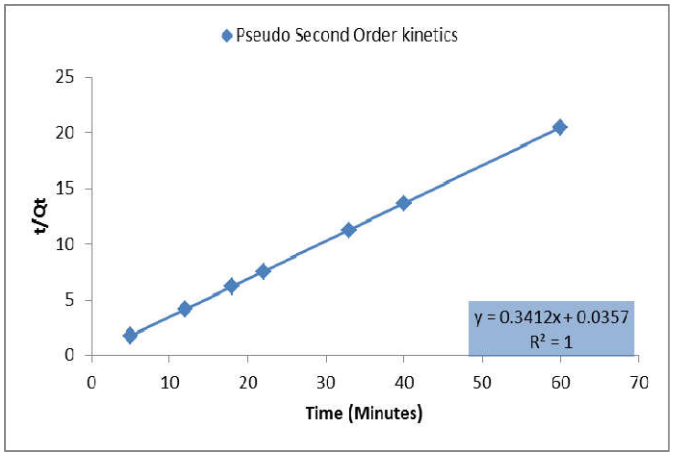

Figure 12. Graph between t/Q_t and Time

The parameter Q_e value was evaluated to be 2.93mg.g^{-1}. The rate constant k_2 was calculated to be 3.26g.mg^{-1}min^{-1}.

Intraparticle Diffusion Model

Weber and Morris based theory of Intraparticle diffusion model is represented as:

$$q_t = k_p t^{0.5} + C \quad \text{..... (15)}$$

Where k_p ($mg.g^{-1}min^{0.5}$) is the intraparticle diffusion rate constant and C represents the width of the boundary layer ($mg.g^{-1}$). A graph between q_t and $t^{0.5}$ was used to evaluate the values of k_p (Wojciech *et al*., 2014).

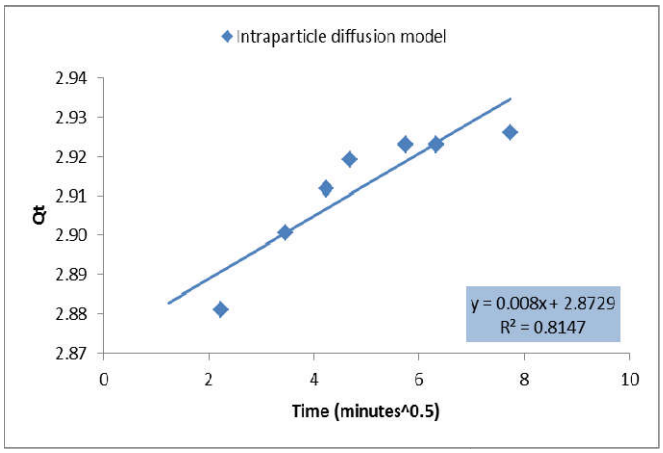

Figure 13. Graph of Intraparticle diffusion model

From Figure13 it was estimated that there was no absolutely linear relationship rather it has an R^2 coefficient of 0.8147. The intraparticle diffusion rate constant was calculated to be $8.0x10^{-3}mg.g^{-1}$ $min^{0.5}$. According to this theory, if the straight line of Q_t against $t^{0.5}$ passes through the origin, then intraparticle diffusion is in command of adsorption. The obtained line was not absolutely straight moreover it was not passing through the origin that indicates that the rate controlling step was not only intraparticle diffusion. The value of C was determined to be 2.8729 $mg.g^{-1}$which present an thought of the width of boundary layer, indicating that the width of the boundary layer increases linearly with the magnitude of intercept (Wojciech *et al*., 2014).

Boyd Kinetic Model

The adsorption mechanism is not fully governed by the diffusion as can be seen in the Figure 13 that the line does not pass through the origin therefore to investigate the adsorption sluggish step, the Boyd model was employed to investigate kinetic data.

$$F = 1 - \frac{6}{\pi^2}\exp(-B_t) \quad \text{..... (16)}$$

$$F = \frac{Q_t}{Q_e} \quad \text{..... (17)}$$

Where Q_e (mg/g) represents equilibrium capacity of adsorption and Q_t ($mg.g^{-1}$) represents adsorption at specified time t. The portion of solute adsorbed at any time t is denoted by F and B_t represents mathematical variable of F. Solving the above two equations (16) and (17) we get

$$B_t = -0.4977 - \ln(1 - F) \quad \text{..... (18)}$$

A graph between B_t and time 't' was plotted but the linear line was not passing through the origin that show external mass transport primarily govern tartrazine adsorption over the nanocomposites where diffusion of particle was the slowest step (Ramachandra *et al*., 2014).

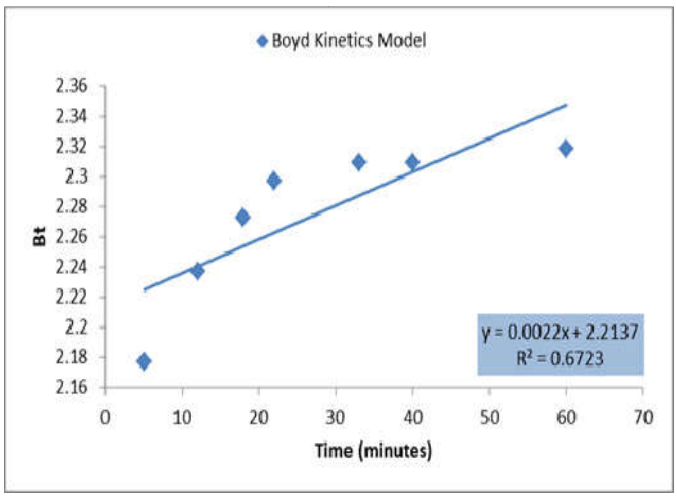

Figure 14. Graph of Boyd's Kinetic Model.

Elovich Model

This is an important model to illustrate the chemisorptions. The model is mathematically represented as.

$$Q_t = \frac{1}{b}\ln(ab) + \frac{1}{b}\ln t \quad \text{..... (19)}$$

The initial sorption rate ($mg.g^{-1}.min^{-1}$) is denoted by 'a'. The level of facade coverage and energy of activation is represented by 'b' ($g.mg^{-1}$).The amount adsorbed at time't' (min) is denoted by 'Q_t' ($mg.g^{-1}$). The constants were evaluated by plotting Q_t against time't'.

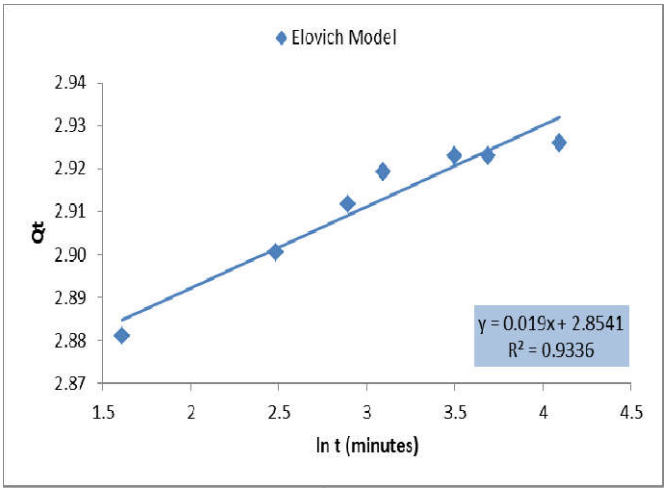

Figure 15. The graph of Elovich Model

From the Figure 15, the constant 'a' was evaluated to be $3.28x10^{63}$ $mg.g^{-1}min^{-1}$and 'b' was determined as $52.63g.mg^{-1}$ respectively.

pH at point of zero charge

pH_{pzc} was evaluated by plotting the final pH after 24 hours and 48 hours against the initial pH. The curves intersect at 6.2 which indicates that at this pH value, the surface charge was neutral and below this pH value, the adsorbent possess positive charge and higher than this pH value, the nanocomposites surface possess overall negative charge as shown in Figure 16.

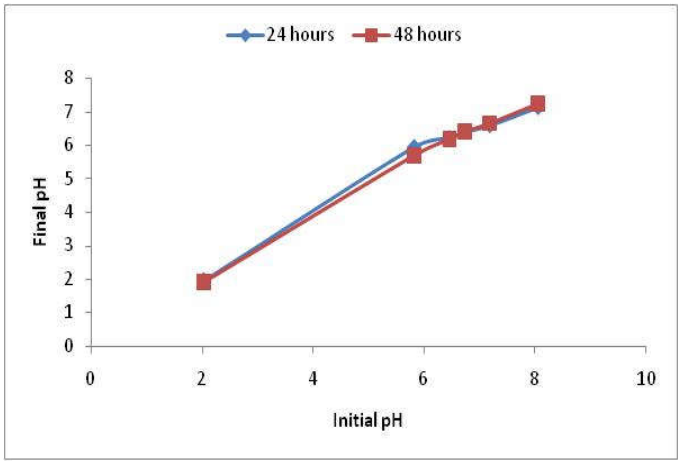

Figure 16.Plot of initial pH versus Final pH at24 hours and 48 hours

Conclusion

Nanocomposites of SnO-CoO were synthesized by a reported method. The characterization of the prepared nanocomposites was carried out by Fourier Transformed Infrared Spectroscopy and Scanning Electron Microscopy. The adsorption of tartrazine dye was studied by using SnO-CoO nanocomposites working as adsorbent under various conditions. The optimum conditions for the adsorption of tartrazine dye on SnO-CoO nanocomposites were determined. The optimum initial concentration was found to be 20ppm, the optimum adsorbent amount was evaluated to be 0.3g and the optimum stay time was determined to be 60 minutes. The experimental data indicate the adsorption obeys pseudo second order kinetics. The data also fitted well in Freundlich isotherm with n values of 1.0154, 1.1061 and 1.0302 at 298K, 313K and 323K respectively. The negative ΔG^o value indicates the spontaneity of adsorption. Other rate determining factors were also taking their part along with diffusion as it was revealed by intraparticles diffusion model with k_p value of be $8.0x10^{-3}mg.g^{-1}min^{0.5}$. pH_{zpc} value was determined to be 6.2. The maximum removal of tartrazine dye by our experimental results was found to be 87.78%, so we can conclude that this specific method can be employed on industrial scale for waste minimization.

REFERENCES

Abbas, M., Hamed, D. and Mehdi, B. 2014. Fast removal of malachite green dye using novel superparamagnetic sodium alginate-coated Fe_3O_4 nanoparticles, *Int. J. of Biolog. Macromol.,* 69: 447-455.

Abdollah, S., Rahman, H., Saied, S. and Hussein, M. 2007. Nanomolar detection of hydrogen peroxide on glassy carbon electrode modified with electrodeposited cobalt oxide nanoparticles, *Analytica Chimica Acta.* 594: 24–31

Baolin, H., Juei, J. T., Kong, Y. L. and Hanfan, L. 2004. Synthesis of size controlled Ag nanoparticles. *Jour. of Mol. Cat. A: Chem.,* 221: 121-126.

Bin F., Guang-Feng W., Mao-Guo L., Ying-Chun G. and Xian-Wen K. 2005. Preparation and application of gold electrode modified with silver nanoparticles and L-Cysteine. *Chem. Anal.,* 50(2): 419-428.

Chunbu, R., Yonghai, S., Zhuang, L. and Guoyi, Z. 2005. Hydrogen peroxide sensor based on horseradish peroxidase immobilized on a silver nanoparticles/cysteamine/gold electrode, *Anal. Bioanal. Chem.,*381, 1179-1185.

Chunjiao, Z., Wenjie, Z., Mingxia, X., Weichang, Z., Qiang, W., Kun, P. and Bingsuo, Z. 2013. Synthesis of Poly(acrylic acid) Coated-Fe_3O_4 Superparamagnetic Nano-Composites and Their Fast Removal of Dye from Aqueous Solution, *Jour. of Nanosci.and Nanotech.,*13(7): 4627-4633.

Dada, A. O. Olalekan, A. P., Olatunya, A. M. 2012. Langmuir, Freundlich, Temkin and Dubinin–Radushkevich Isotherms Studies of Equilibrium Sorption of Zn^{2+} Unto Phosphoric Acid Modified Rice Husk, *IOSR J. of app. Chem.*,3(1): 38-45.

Feray, B., Oral, L. and Hanifi, S. 2013. A novel low temperature sol–gel synthesis process for thermally stable nano crystalline hydroxyapatite, *Powder Tech.,*233, 295-302.

Gajendiran, J. and Rajendran, V. 2014. Synthesis and characterization of coupled semiconductor metal oxide (ZnO/CuO) nanocomposite, *Mat. Lett.,*116, 311-313.

Guang-Feng, W., Mao-Guo, L., Ying-Chun, G. and Bin, F. 2004. Amperometric Sensor used for determination of thiocyanate with a Silver Nanoparticles Modified Electrode, sensors, 4(9): 147-155.

Hajira, T., Uroos, A. 2014. Lignocellulosic: Non-Conventional Low Cost Biosorbent for the Elution of Coomassie Brilliant Blue(R-250), *Int. J. of Chem.,*6(2), 56-72.

Hamid, T., Majid, J., Mehdi, R. and Ali, S. 2013. A high activity adsorbent of ZnO-Al_2O_3 nanocomposite particles: Synthesis, characterization and dye removal efficiency, *app. Sur. Sci.,*276, 317-322.

Irena,M., Abdurauf, P., Toma, G. and Ljubomir, A.2006. Electrochemical polymerization of aniline in presence of TiO_2 nanoparticles. bull. of the Chem. and *Tech. of Mac*., 25(1): 45-50.

Juan, C., Juchuan, L., Liu, L., Anjian, X., Shikuo, L., Lingguang, Q., Yupeng, Y. and Yuhua, S. 2014. One-pot synthesis of novel Fe_3O_4/Cu_2O/PANI nanocomposites as absorbents in water treatment, *J. Mater. Chem*., A. 2(21): 7953-7959.

Khizar, H., Mazen, M. K., Shakeel, A. 2011. Effect of operational key parameters on photocatalytic degradation of phenol using nano nickel oxide synthesized by sol–gel method, *Journal of Molecular Catalysis* A: Chemical.,336: 64-71.

Khizar, H., Mazen, M.K., Shakeel, A. and Ahsan, M.S. 2011. Nano ZnO synthesis by modified sol gel method and its application in heterogeneous photocatalytic removal of phenol from water, Applied Catalysis A: General. 393: 122-129.

Kumar, A., Chaudhary, P. and Verma, P. 2013. Adsorption of Reactive Red 194 Dye from Textile Effluent by Using Class F Fly Ash, *Sch. J. App. Med. Sci.,*1: 111.

Lihua, Y., Jun, Z., Ping, Z., Jiaxing, C., Ruoyu, W., Tingtin, W., Yun, L., Xuemin, Z. and Huijun, J. 2011. Electrochemical sensor based on molecularly imprinted membranes at platinum nanoparticles-modified electrode for determination of 17β-estradiol. *Biosen. and Bioelect*.,29(1): 29-33.

Manigandan, R., Giribabua, K. and Suresh, R. 2013. Cobalt Oxide Nanoparticles: Characterization and its Electrocatalytic Activity towards Nitrobenzene, *Chem. Sci. Trans.,* 2(S1), S47-S50.

Mao-Guo, L., Ying-Chun, G., Xian-Wen, K., Guang-Feng, W. and Bin, F. 2005. Effect of Ag nanoparticles for electrochemical sensing of brilliant Cresyl Blue, *Chem. Let.,* 34(3): 386-387.

Mirjalili, F., Hasmaliza, M. and Chuah, A. 2010. Size-controlled synthesis of nano α-alumina particles through the sol–gel method, *Ceramics International*, 36: 1253-1257.

Mohammad, I., Chan, W. and Haliza, R. 2013. Freundlich Isotherm Equilibrium Equastions in Determining Effectiveness a Low Cost Absorbent to Heavy Metal Removal In Wastewater (Leachate) At TelukKitang Landfill, PengkalanChepa, Kelantan, Malaysia, *J. of Geo. and Earth Sci.,*1(1), 1-8.

NIIR Board. 2004. The complete technology book on dyes and dye intermediates.

Nikolina, A. T., George, Z. K., Nikolaos K. L. and Eleni A. D. 2013. Functionalization of Graphite Oxide with Magnetic Chitosan for the Preparation of a Nanocomposite Dye Adsorbent, Langmuir, 29(5), 1657-1668.

Nirasttisai, R., Wisitsree, W., Charun, B. and Juntima, C. 2010. Synthesis of Fe/MgO nano-crystal catalysts by sol–gel method for hydrogen sulfide removal, *Chem. Eng. Jour*., 162(1): 84-90.

Ramachandra, M. and Girish, C.R. 2014. Adsorption of Phenol from Aqueous Solution Using Lantana camara, Forest Waste: Kinetics, Isotherm, and Thermodynamic Studies, *Int. Sch. Res. Not.,* 2014: 1-16

Saeedeh, H. and Mohammad, R. S. 2013. Novel Ag/Kaolin Nanocomposite as Adsorbent for Removal of Acid Cyanine 5R from Aqueous Solution, *Jour. of Chem.,* 2013: 1-7.

Srivastava, V., Sharma, Y. C. and Sillanpaa, M. 2015. Application of nano-magnessoferrite (n-$MgFe_2O_4$) for the removal of Co^{+2} ions from synthetic waste water: kinetic equilibrium and thermodynamic studies. *App. Sur. Sci.,* 338, 42-54.

Sumanjit, K., Seema, R. and Rakesh, K.M. 2013. Adsorption kinetics for the removal of hazardous dye congo red by biowaste materials as adsorbent, *Jour. of Chem.,* 2013, 1-12.

Sumita, G., Asish, S., Mohammad, R., Asit, B.P., Holger, S. and Sagar, P. 2014. Enhanced removal of methylene blue and methyl violet dyes from aqueous solution using a nanocomposite of hydrolyzed polacrylamidegrafted xanthan gum and incorporated nanosilica. ACS Appl. Mater. Interfaces, 6 (7): 4766–4777.

Sushanta, D., Jacob, K. and Maurice, S. O. 2014. Removal of Congo red from aqueous solution by two variants of calcium and iron based mixed oxide nano-particle agglomerates*, J. of Ind. and Eng. Chem.,*20(4), 2119-2129.

Vijayaprasath, G., Ravi, G. and Hayakawa, Y. 2013. Effect of Solvents on Size and Morphologies Of SnO Nanoparticles via Chemical Co-precipitation Method, *Int. J. of Sci. and Eng. App.,* Special Issue, NCRTAM ISSN-2319-7560.

Vinod, K. G., Deepak, P. and Gaurav, S. 2014. Polyaniline zirconium (IV) silicophosphate nanocomposite for remediation of methylene blue dye from waste water*, Jour. of mol. Liq.,* 190, 139-145.

Wojciech, K., Iwona, P., Ewa, M. and Izabella, J. 2014. Adsorption Kinetics of Acid Dye Acid Red 88 onto Magnetic Multi-Walled Carbon Nanotubes-Fe_3C Nanocomposite Adsorption Acid Red 88 onto Magnetic Multi-Walled Carbon Nanotubes-Fe_3C Nanocomposite, *Clean-Soil, Air, Water,* 42(3): 284-294.

Xiaoli, Z., Xin, G., Jing, W., Ting, C. and Genxi, L. 2005. A new reduction route of hypoxanthine and its nonenzymatic detection based on silver nanoparticles. *Jour. of Mol. Cat. A: Chem.,* 239: 201-204.

Yingju, F., Zhen, L., Le, W. and Jinhua, Z. 2009. Synthesis of starch stabilized Ag nanoparticles and Hg^{+2} recognition in aqueous media. *Nano. Res. Lett.,*4: 1230-1235.

Yuvaraj, H. and Jae-Jin, S.2014. An efficient removal of methyl orange dye from aqueous solution by adsorption onto chitosan/MgO composite: A novel reusable adsorbent, *App. Sur. Sci., 292*, 447-453.

Zhonghui, C., Jianan, Z., Jianwei, F., Minhuan, W., Xuzhe, W., Runping, H. and Qun, X. 2014. Adsorption Of methylene blue onto poly(cyclotriphosphazene-co-4,4-sulfonyldiphenol) nanotubes: Kinetics, Isotherm and thermodynamics analysis*, J. of Hazard. Mat.,* 273: 263-271.

****